CONVECTIVE HEAT TRANSFER IN ROOMS

Hatton, A and Awbi, H B

Department of Construction Management & Engineering

University of Reading

UK

ABSTRAC

Data for convective heat transfer coefficients (CHTC's) published in the literature tend to be for an isolated heated vertical plate, with few data based on measurements at room surfaces Accurate values of CHTC's for internal room surfáces are needed for heat transfer calculations in buildings using thermal models and also for room air movement calculations using CFD models. Most existing computer models use CHTC's that have been calculated for isolated surfaces.

This work presents accurate convective heat transfer coefficients for a heated wall in a room. Using heating plates attached to a wall of an environmental test chamber and by accurately measuring the surfáce and air temperatures, the CHTC's have been deduced afder allowing for conduction and radiation losses from the plates. When compared with data published in the ASHRAE Handbook and the CIBSE Guide, the CHTC's values given in this paper differ by between -13% and + 20% respectively.

INTRODUCTION

Natural Convection, Radiation and Conduction are the heat transfer mechanisms occurring from the surfaces of a building. Under non-ventilated conditions, heat is convected to the indoor air as a result of the temperature difference between the building's surfaces. Many heat transfer calculations within buildings are performed using a heat transfer coefficient which is a combination of convection and long wave radiation {1,2}. Convective heat transfer depends upon the direction of heat flow into or out of the surface, the temperature difference between the surface and air, as well as geometry and surface texture {3,4}. Inter-surface radiation is a function of the temperature of the room surfaces, surface emmissivity, visual contact between surfaces (view factor) and the reflectivity of the surfaces. These fundamental heat transfer concepts have been used for formulating various theories for calculating the heat exchange within buildings {5}.

A literature survey has shown that there is a lack of reliable data for convective heat transfer coefficients relating to room surfaces. A number of research papers {6 - 11} have presented results for room surfaces, most of which dealt with real size rooms and the others {7,8} investigated tests carried out in small water filled boxes.

For a wall within an enclosure, the CHTC's reported were found to vary over the range 1.6 to 5 W/m^2K at a surface to air temperature difference of 15K. The difference can be attributed to the fact that few researchers have accounted for the effect of thermal radiation in their calculations. It is clear that radiative heat transfer is significant enough to be included in the heat transfer process, however the use of a low emmissivity surface such as aluminium would reduce the radiative heat flux, but would not eliminate it. Aluminium has been used by some authors in their work {8,11}. Other areas where inaccuracy occurs is in the instrumentation used. In some work thermocouples have been used to measure the temperatures often with an accuracy of ±1K at best. This error in temperature measurement could become significant in rooms where the temperature difference between internal surfaces and air is usually only a few degrees.

This paper presents results for CHTC of a heated surface adjacent to a cool wall. Both mean values and local variations of CHTC on the wall are given here. The data is compared with the current values published in the CIBSE Guide {1} and the ASHRAE Handbook {12} for isolated plates and with room surface data from Khalifa and Marshall {11}.

DESCRIPTION OF THE TEST CHAMBER

The test chamber was constructed by Procema Ltd and is located in the Engineering Building of Reading University. The chamber has external dimensions 4m x 3m x 2.523m and is constructed using panels with dimensions 1.2m x 3m x 0.113m for the floor, 1.2m x 3m x 0.11m for the ceiling and 1.2m x 2.3m 0.11m for the walls.

The panels are constructed from 9mm plywood (12mm for the floor), 100mm of polystyrene board and a steel plastic coated plate (stelvatite). Floor joists support the chamber 300mm from the laboratory floor.

The interior of the chamber comprises of two compartments divided by a 9mm thick plywood partition. One compartment is equipped with a cooling coil and a fan. The refrigeration is provided by a compressor housed outside the chamber which is capable of cooling the compartment to -5°C and also heating it to 35°C if required. The second compartment is the main experimental area with interior dimensions 2.78m x 2.78m x 2.3m (ceiling height).

Four - wire Platinum Resistance Thermometer (PRT) sensors (accuracy = ±0.15K) have been fixed to the inside (Fig. 1) and outside surfaces of the chamber. Other measuring devices used in the tests were a Wattmeter and an Infra Red Imaging Camera. Surface heating was provided by heating plates controlled by a PID temperature controller.

DESCRIPTION OF THE HEATING PLATES

The plates (Figs. 2 & 3) were constructed from a 2mm sheet of polished aluminium, a Flexel sheet heating element and a 6mm thick panel of plywood. Holes of approximately 5mm were drilled into the aluminium for housing the PRT sensors used to measure the surface temperature. To allow for the PRT cable, grooves were milled into the back of the aluminium plates.

Five plates with dimensions 2.28 x 0.52m were used to heat the wall adjacent to the cold wall (Figs. 1 & 2). Ten PRT sensors were used to measure the surface temperature of the plates with another 9 attached to steel wires fixed vertically to the ceiling and floor 10cm {13} from the heated surface. These measured the temperature at the air edge of the air boundary layer and were shielded for radiation. One surface temperature sensor was used for controlling the plate temperature using a temperature controller.

DESCRIPTION OF THERMAL IMAGING CAMERA

An infrared camera (IR) converts electromagnetic thermal energy radiated from an object into electronic video signals. These signals are amplified and transmitted via an interconnecting cable to a monitor where the signals are further amplified and the resultant image is displayed on the screen. A scanner measures the infrared radiation within a certain spectral range. Since the received radiation has a non-linear relationship to the object temperature, it can be affected by atmospheric damping and also includes reflected radiation from the object surroundings. To reduce the errors caused by these effects the camera must be placed close to the investigated object with surroundings of low thermal radiation emission .

An Agema 870 IR camera was used primarily to measure the emmissivity of the aluminium plates and the plywood interior of the chamber and also to investigate the plate surface temperature variation and the effect the cold wall has on plate temperature distribution.

DETERMINATION OF THE HEAT TRANSFER COEFFICIENT

To deduce the heat flux into the chamber, Q_{in}, the conduction loss from the heated wall to the outside was first calculated using:

$$Q_{in} = P - kA(T_{in} - T_{out})$$

$$Q_{in} = Q_r + Q_c$$

then by calculating the radiative heat flux using:

$$Q_r = \frac{A\varepsilon[\sigma T^4 - Q_j]}{1-\varepsilon}$$

$$Q_c = Q_{in} - Q_r$$

Therefore the CHTC can be found using:

$$h_c = \frac{Q_c}{A(T_s - T_a)}$$

A computer program has been devised to undertake these calculations for each position on the plates. The calculations for the radiosity were carried using a computer program which solves the radiation matrices using the Gauss-Seidel method. Further details can be found in reference {14}.

EXPERIMENTAL PROGRAMME

Test for a Heated Wall Adjacent to a Heat Sink

The results presented in this paper were obtained for a heated wall adjacent to a cooled wall (heat sink). The plates where heated to 25°C and the adjacent wall was cooled to 15°C. The chamber was then left running overnight and the temperatures and the power consumed by the plates were measured and logged every 10 minutes. This process was repeated

with 5K increases in the plate temperatures and 5K decreases in the cool wall temperature. The aim was to keep a constant room air temperature ≅ 20°C so as to produce the required temperature difference between the plate and ambient.

The logged data from the tests was then dissected into various regions and the data for the steady state condition was used in the calculations. The CHTC's were then obtained using the computer program described earlier.

Tests for Isolated Plates

Tests were also carried out to further investigate the heat transfer process for a heated section of a wall. These are:

1. One plate (No.3) heated to 45°C in the centre of the wall, with 5 PRT's fixed onto the plate and 5 suspended 10cm away, to measure the surface and air temperatures at the edge of the boundary layer. Two wooden panels were placed at either side of the plate to effectively isolate the cross convection. The cool compartment was chilled to 5°C and the chamber was then allowed to attain a steady state. The temperature and power were logged as with the earlier tests and the data pertaining to the steady state region was extracted.

2. Step 1 was repeated with plate 1 heated (plate directly adjacent to the cool wall), plate 5 (plate furthest from the cool wall) and the case when plates 3 & 4 where jointly heated.

The calculations were dealt with in the same manner as for the whole wall tests, however, because the area of the heated plates is small in comparison with that for other room surfaces, Q_r in this case was computed using:

$$Q_r = \varepsilon A \sigma (T_s^4 - T_{mean}^4$$

i.e. a view factor of 1 has been assumed here.

Tests with the Infra Red Camera

The emmissivity of aluminium generally varies between 0.039 and 0.07 {15} depending upon the purity of the alloy and the corrosion of the surface. This difference would result in an error in the value of CHTC deduced from measurements. However using the IR camera, actual emmissivities were found for the plates and used in the heat transfer calculations.

Also the heat distribution over the heated plates and other chamber surfaces was examined using the IR camera to shed more light on the temperature distribution on the surfaces.

RESULTS

Infra-Red Camera

Using the IR camera several tests were undertaken to find the emmissivity of the heating plates. By comparing the emmissivity of the plate surface with a patch covered by an adhesive tape of known emmissivity, an average value of:

$$= 0.061 \pm 5\%$$

was then calculated and used in the heat transfer calculations.

Figure 4 shows an image of the temperature variation over the plates as recorded by the IR camera for a surface to air temperature difference $\Delta T \cong 37°C$. It can be seen that plate 1, which is the plate to the left on the image, is clearly the coolest one because of its proximity to the cool wall. The surface temperatures of the other plates increase with increasing height and distance from the cool wall. Comparing this image with Fig. 5, which represents the temperature of the plates as measured by the PRT sensors, similar temperature variations can be seen. The apparent 'hot' lines in Fig. 4 are the gaps between the plates were the emmissivity value of the plywood wall is much higher than that of the aluminium plates, hence these gaps represent "higher" thermal emission.

Whole Wall Heated

The mean heat transfer coefficient for a uniformly heated wall is presented in Fig. 6. The key in this Figure represents the locations of the measuring points on the wall. Geometric regression gives the following correlation for the mean CHTC:

$$h_c = C (\Delta T)^n$$

where C and n are constants. The values of C and n are given in Table 1 for each location on the heated surface. The scatter band for CHTC's with ΔT, shown in Figure. 6, is limited by the values for points 1 and 8 as the upper limit and points 4 and 7 as the lower limit. The values for the other points lie within this band.

Isolated Plates

When plotting the local heat transfer coefficient with height, see Fig. 7, the general shape of the line appears to be a ' tick' . When plate 3 alone is heated in isolation it is clear that between a height of 0.24m and 0.69m the CHTC falls with an increase in height and then begins to rise linearly with height after this

point. This correlation is apparent in each case observed except when plate 1 is heated in isolation. For this plate which is fixed directly adjacent to the cool wall, the CHTC is almost constant over the height between 0.24m and 0.69m and then gradually increases after this. The behaviour of this plate could be due to the cooling of the adjacent wall which produces a more even temperature distribution over the surface of the plate.

Generally, the CHTC's for plate 3 are higher than those of the other plates investigated; the lowest being those for plate 4 when plates 3 and 4 were both heated.

Smoke tests carried out in the boundary layer of the isolated plates showed that the flow was laminar around the bottom of the plate followed by, a transition region at a height of approximately 0.7m, above which the flow was seen to become turbulent. By using the Grashof number range for laminar flow ($<1.5 \times 10^9$) {16} the height of the transition was calculated to be approximately 0.7m. In Fig. 7 it can be seen that CHTC's fall with height in the laminar region, but increase with height in the turbulent region.

Average CHTC's can be calculated for both laminar and turbulent regimes from the data collected as given below:

$$h_c = 1.49\ (\Delta T)^{0.345}$$

for turbulent flow.

$$h_c = \ .667\ (\Delta T)^{0.289}$$

for laminar flow

For the heat transfer coefficient versus temperature difference over the isolated plates, the results show a linear relationship between the CHTC and the temperature difference with a negative slope, see Fig. 8. Plate 3 has the highest CHTC value over the range of temperature differences measured, however plates 3 and 4 have the lowest values when they are jointly heated. Plates 1 and 5 are the end plates and the data for these lie along the same region on the graph.

Comparison with Published Data

A comparison between the average CHTC over the whole surface with equations commonly quoted in handbooks (e.g. ASHRAE Handbook {12} and CIBSE Guide {1}) is shown in Fig. 9. An equation found by Khalifa and Marshall {11} for a heated wall in an enclosure has also been included. The correlation found for the heated wall (Equation 10 in Table. 1) lies in the range of values between the ASHRAE / Khalifa data and the CIBSE data. The CHTC's values produced in this work lie within the extreme values found in the literature and presented in Fig. 9. The spread of the data from the literature makes further conclusions difficult to draw. However, the values for walls seem to be higher than those for isolated surfaces.

CONCLUSIONS

This study was carried out to investigate the heat transfer from a partially and fully heated wall adjacent to a cool wall in an enclosure and led to the following conclusions.

For a surface to air temperature difference range of 5 to 25 K and a vertical wall height of 2.3m, an equation for the mean CHTC was found to be:

$$h_c = 1.572\ (\Delta T)^{0.307}$$

The CHTC is found to vary over the surface with respect to height, whereby the CHTC falls with increase in height in the lower (laminar) region but increases in the upper (turbulent) region.

3. The heat transfer from the heated surface close to the cool wall show a minimal dependence upon height. The dependence increases with an increase in horizontal distance from the cool wall.

4. Comparisons with published results suggest that the CHTC equation produced here gives generally higher values than those for isolated surfaces, but lies within the range of values quoted for enclosures.

Further work is currently in progress to study the heat transfer from a heated wall opposite a cool wall, as well as a ceiling and a floor within the same test chamber. More work will also be undertaken by introducing air movement in the chamber to study it's effect on the convective heat transfer from the chamber surfaces.

ACKNOWLEDGEMENT

This work is supported by the Engineering and physical Sciences Research Council, UK under Grant Reference GR/J47606.

REFERENCES

1 CIBSE Guide Section A5 and A9 (1979 and 1986), Chartered Institute of Building Services Engineers, London.

2 Uttenbroek, J (1990), Building heat loss calculations: Choice of internal temperature and of heat transfer coefficient hi, *Building Serv. Eng. Res. Technol.* **11**(2), 49 - 56.

3 Alamdari, F and Hammond, G P (1983), Improved correlations for Buoyancy-driven convection in rooms, *Building Serv. Eng. Res. Technol.* **4**(3),106 - 112.

4 Khalifa, A J N and Marshall, R H (1989), Natural and forced convection on interior building surfaces: Preliminary results, *Proc. Applied Energy Research Conf.*, Swansea, pp249 - 257

5 Steffanizzi, P, et al (1990), Internal long wave radiation exchange in buildings: Comparison of calculation methods: I - Review of algorithms II - Testing of algorithms, *Building Serv. Res. Technol.* **11**(3), 81 - 96.

6 Min T C, Schutrum L F, Parmelee G V and Vouris J D (1956), Natural convection and radiation in a panel heated room, ASHRAE Trans 62, 337 - 58.

7 Bohn M S, Kirkpatrick A T, Olson D A (1984), Experimental study of three - dimensional natural convection high-Rayleigh number, *Journal of Heat Transfer*, **106**, 339 - 345.

8 Bauman F, Gadgil A, Kammerud R, Greif R (1980), Buoyancy-driven convection in rectangular enclosures, ASME Paper No. 80 - HT - 66.

9 Qingyan C, Meyers C A, van der Kooi J (1989), Convective heat transfer in rooms with mixed convection, *International seminar on indoor air flow patterns held at Laboratory of Thermodynamics*, University of Liege, Belgium, 14pp.

10 Delaforce S R, Hitchen E R, Watson D M T (1993), Convective heat transfer at internal surfaces, *Building and Environment*, **28**, 211 - 220.

11 Khalifa A J N, Marshall R H (1990), Validation of heat transfer coefficients on interior building surfaces using a real - sized indoor test cell, *Int. Journal of Heat and Mass Transfer*, **33**, 2219 - 2236.

12 ASHRAE Fundamentals (1981), *American Society of Heating, Refrigeration and Air-conditioning Engineers*, Atlanta, GA.

13 Irving A D, Dewson T, Hong G, Day B (1994), Time series estimation of convective heat transfer coefficients, *Building and Environment*, **29**, 80 - 96.

14 Awbi H B and Gan G (1991), Computational fluid dynamics in ventilation, *Proc. of CFD for Environmental and Building Services Engineer,* 67 - 79, Institution of Mechanical Engineers, London.

15 Janna W S (1986), *Engineering Heat Transfer*, PWS Publishers, Boston.

16 Mahajan R L, Gebhart B (1979), An experimental determination of transition limits in a vertical natural convection flow adjacent to a surface, *J. Fluid Mech.*, **91**, pp. 131 - 154.

17 Rogers G F C, Mayhew Y R (1967), *Engineering Thermodynamics Work and Heat Transfer*, Longmans.

NOMENCLATURE

ε	emmissivity of the heated plates
σ	Stefan-Boltzmanns constant, W/m^2K^4
h_c	CHTC, W/m^2K
A	area of the heated surface, m^2
P	power consumed by the panels, W
Q_c	convective heat flux, W
$Q_j^{"}$	radiosity associated with the heated surface, W/m^2
Q_r	radiative heat flux, W
T_a	air temperature at the edge of the boundary layer, °C
T_{in}	internal surface temperature of the heated wall, °C
T_{mean}	mean radiant temperature, K
T_{out}	outside surface temperature of the heated wall, °C
T_s	surface temperature of the plates, K or °C

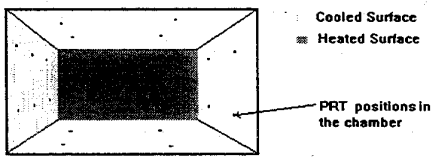

Fig. 1 Inside view of the chamber facing the heated wall.

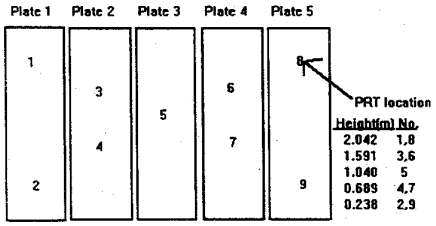

Fig. 2 Plate alignment on the wall and positions of temperature sensors.

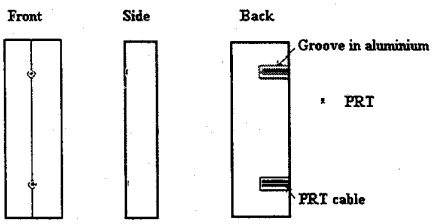

Fig. 3 PRT installation in aluminium plate.

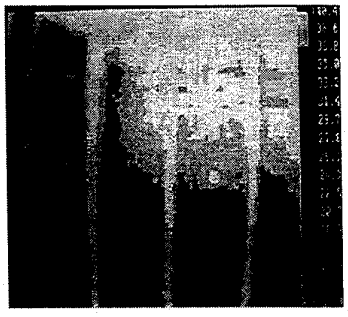

Fig.4 Thermal image of a heated wall taken by the IR camera

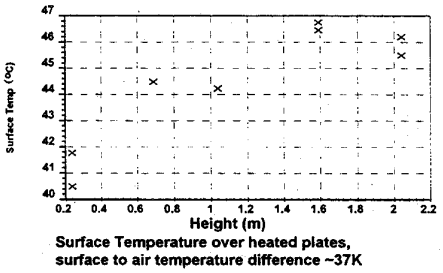

Figure 5

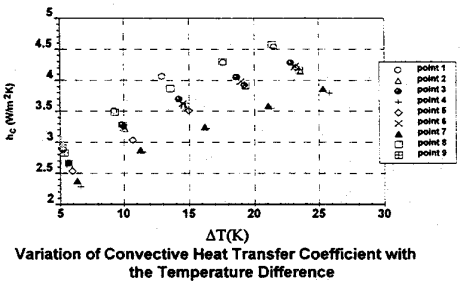

Figure 6

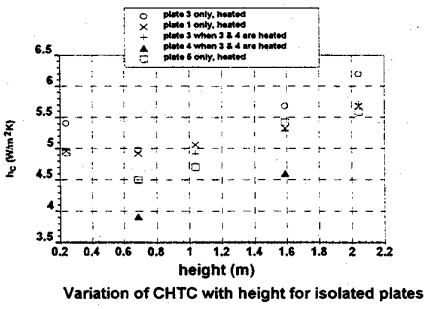

Figure 7

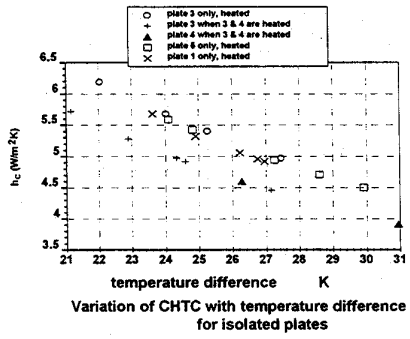

Figure 8

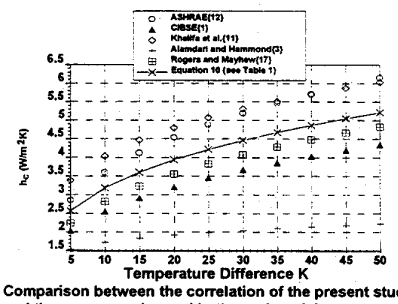

Comparison between the correlation of the present study and those commonly used in thermal models

Figure 9

Table 1 Correlation equations for the CHTC at different locations on the heated wall.

Equation No.	PRT Location/Region	Heat Transfer Coefficient (W/m^2K)	Standard Deviation
1	1	$h_c = 1.704(\Delta T)^{0.324}$	± 1.49%
2	2	$h_c = 1.521(\Delta T)^{0.32}$	± 0.64%
3	3	$h_c = 1.48(\Delta T)^{0.343}$	± 0.74%
4	4	$h_c = 1.137(\Delta T)^{0.372}$	± 0.43%
5	5	$h_c = 1.27(\Delta T)^{0.378}$	± 1.34%
6	6	$h_c = 1.512(\Delta T)^{0.328}$	± 0.50%
7	7	$h_c = 1.24(\Delta T)^{0.349}$	± 0.61%
8	8	$h_c = 1.712(\Delta T)^{0.32}$	± 0.67%
9	9	$h_c = 1.813(\Delta T)^{0.259}$	± 0.87%
10	Whole Wall	$h_c = 1.572(\Delta T)^{0.307}$	± 8.9%
11	Laminar	$h_c = 1.67(\Delta T)^{0.289}$	± 14.9%
12	Turbulent	$h_c = 1.602(\Delta T)^{0.328}$	± 3.7%